PERGAMON

Solid State Communications 120 (2001) 59–63

solid state communications

www.elsevier.com/locate/ssc

Vortex dynamics in $Bi_2Sr_2CaCu_2O_{8+\delta}$ single crystals with planar defects

J.A. Herbsommer, V.F. Correa, G. Nieva, H. Pastoriza*, J. Luzuriaga

Centro Atómico Bariloche and Instituto Balseiro, CNEA and UNC, 8400 Bariloche, Argentina

Received 28 July 2001; accepted 6 August 2001 By M. Cardona

Abstract

We have studied the effects of *c*-axis correlated planar defects on the vortex lattice of $Bi_2Sr_2CaCu_2O_8$ single crystals using Bitter decoration, transverse ac permeability and X-ray measurements. Our results show that the low field low temperature phase coherent vortex lattice exhibits anisotropic pinning in the presence of these planar defects. Frequency dependent ac permeability measurements show that the ordered solid–liquid transition is first order as in samples free of correlated defects. However, the melting point is detected only when the excitation field is along the defects.

PACS: 74.60.Ge; 74.62.Dh

Keywords: A. High-T_C superconductors; D. Flux pinning and creep; B. Crystal growth

1. Introduction

High Temperature Superconductors (HTSC) have a very complex magnetic field-temperature (H–T) phase diagram. Several factors contribute to this: the anisotropic properties arising from their layered structure, the competition between pinning and elastic energy, and the relatively large thermal fluctuations. The pinning force (and consequently the critical current J_c) additionally depends on the kind, strength, density and dimensionality of the sample defects that act as pinning centers of the vortex structure.

Correlated defects in HTSC modify not only the critical current but also the H–T phase diagram of these materials. The effect is clearly observed in $YBa_2Cu_3O_{7+\delta}$ (YBCO) where artificially produced defects of columnar geometry produce large enhancements of J_c [1]. In this material the existence of naturally occurring twin boundaries modify the solid phase of the vortex system [2] and can also produce anisotropic vortex dynamics and critical currents [3,4,5].

Columnar defects also enhance the critical current of $Bi_2Sr_2CaCu_2O_{8+\delta}$ (BSCCO), although the effect is different than in YBCO [6]. This is a consequence of the high anisotropy of BSCCO, also responsible for the quantitative differences in the H–T phase diagram with respect to that of YBCO.

This phase diagram has a rather low (~350 Oe) critical decoupling field, H_{cr}, which separates a low field region with phase coherence along the *c*-axis from a disordered quasi-2D phase above H_{cr} [7–10]. A dynamical manifestation of this order–disorder decoupling transition at H_{cr} is the so called second peak effect in the magnetization. At high temperatures the vortex structure is in a liquid phase with no phase coherence in any direction. The liquid to solid phase transition in clean samples is found to be first order below H_{cr}[11,12].

Concerning the average crystallographic structure of BSCCO there are many open questions arising from the variety of local distortions found with transmission electron microscopy [13] (TEM) such as twins, intergrow defects, strain induced monoclinic phase, etc. More recently, several authors have revealed the existence of extended planar defects parallel to the (010) planes in BSCCO [14,15], Pb doped BSCCO [14] and Ti doped BSCCO [16] using different techniques such as TEM, magneto-optic imaging, polarized light, etc. Some of these local structure variations contribute to vortex pinning. Using high-resolution Faraday effect, Koblischka et al. [17] and Yang et al. [18] and using

* Corresponding author. Tel.: +54-2944-445171; fax: +54-2944-445299.

E-mail address: hernan@cab.cnea.gov.ar (H. Pastoriza).

0038-1098/01/$ - see front matter
PII: S0038-1098(01)00349-0

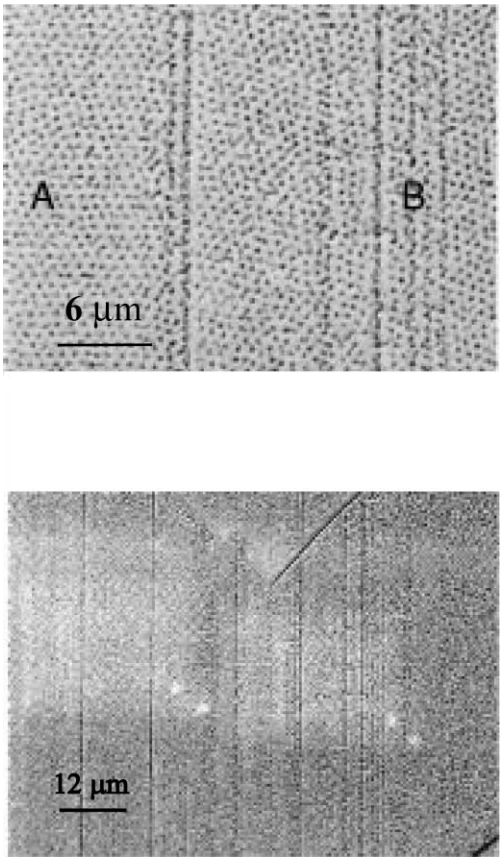

Fig. 1. Upper: Typical image of the pattern obtained in the Bitter decoration at 36.1 Oe. Zones such as A show hexagonal order while in regions like B the order is destroyed by the presence of linear defects. Lower: Region of the surface in which we found a V-shaped terrace in the upper part of the image. Observe that in the higher and the lower part the positions of the defects coincide.

Bitter decoration Fasano et al. [19,20], have shown the existence of planar defects that act as pinning centers in BSCCO. In the Faraday effect measurements, performed in the critical Bean state above H_{cr}, the flux penetrates the sample along the planar defects, while in the Bitter decoration experiments done below H_{cr} and with no applied current, the vortex density is seen to be higher inside the planar defects.

In this paper we study BSCCO with planar defects using Bitter decoration, transverse ac permeability and X-ray measurements. In particular, ac permeability measurements made in the linear regime allow us to explore the H–T phase diagram below and above H_{cr} in a vortex state that is less perturbed than the Bean critical state. Our results show that the phase coherent vortex lattice below H_{cr} exhibits anisotropic pinning in the presence of the planar defects, but that at fields above H_{cr} the response of the *c*-axis uncorrelated vortices to a tilting stress does not depend on the orientation between the tilting stress and the planar defects. Frequency dependence measurements show that the solid–liquid transition is of first order below H_{cr} as in clean samples. However, the melting point is detected only when the excitation is along the defects.

2. Experimental results

The measurements presented in this work were performed on a $Bi_2Sr_2CaCu_2O_{8+\delta}$ (BSCCO) single crystal grown by the self flux method [21]. The dimensions of the crystal were 2 mm × 1.3 mm × 20 μm and the critical temperature $T_c = 86.15$ K.

In Fig. 1 we show an image obtained from a Bitter decoration at 36 Oe. We can observe that the usual pattern of hexagonal symmetry with long range order typically imaged in BSCCO [22] single crystals is strongly modified. The crystalline structure is replaced by a coexistence of an ordered hexagonal lattice, zone A, with regions like B in which the vortices are arranged in rows with a density higher than the average which resemble images of decorations of YBCO with twin boundaries [4,23–28]. The typical distance between vortices along a row is 60–70% of the lattice parameter in the hexagonal lattice (zone A).

It can be observed from the decoration experiment that this line defects are always along one axis of the crystal. They are irregularly spaced with an average distance between defects of 20 μm. X-ray diffraction experiment indicates that the direction of the defects corresponds to the *a* crystal orientation.

The fortuitous existence of steps in the surface of the sample gives us some evidence about the *c*-axis correlation of these defects. In the upper part of the image of Fig. 1 it is clearly seen one of such steps as a V-shaped zone which is elevated about 0.5 μm over the surface of the rest of the

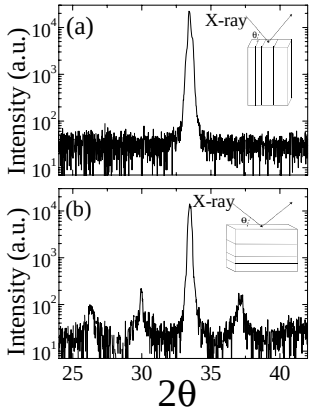

Fig. 2. (a) X-ray diffraction peak corresponding to the (200) direction. The angle θ is measured from the perpendicular to the line defects (see inset). (b) X-ray diffraction peak corresponding to the (020) direction with the angle θ measured from the line defects. Note the satellite peaks related to the superstructure in the *b* direction.

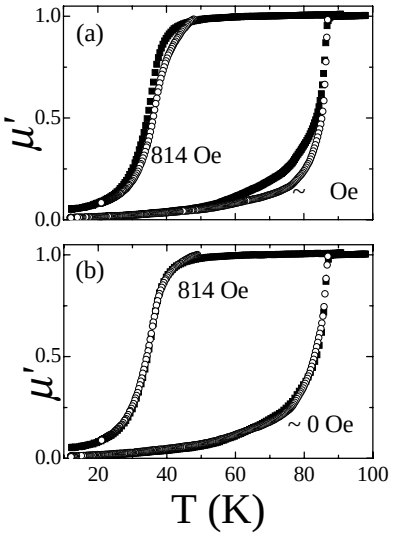

Fig. 3. (a) μ'_{IN} (closed symbols) and μ'_{OUT} (open symbols), see text for definition, as a function of temperature for 0 and 814 Oe. (b) Same data as (a) when μ'_{IN} is corrected by size effect.

crystal. We can observe that the position of the defects in the lower part coincides with the position of the defects in the upper part. This is only possible if the defects extend along the *c*-axis.

Shown in Fig. 2 are the X-ray diffraction data taken with the scattering angle θ measured from a direction perpendicular to the defects (Fig. 2a) and parallel to them (Fig. 2b). We observe the (200) and (020) reflections respectively. The satellites corresponding to the incommensurated structure modulation along the *b* direction [18] are clearly observed in Fig. 2b. This indicates that the defects are in planes along the *a* direction of the crystal. The defects found with magneto-optical techniques have the same crystallographic direction as reported by Yang et al. [18]. We have also performed X-ray diffraction experiments along the

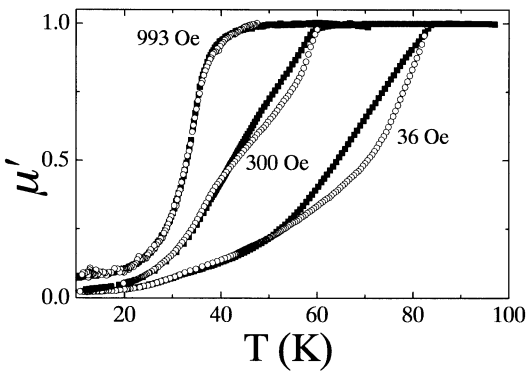

Fig. 4. μ'_{IN} (closed symbols) and μ'_{OUT} (open symbols) for 36, 300 and 993 Oe as a function of temperature.

c-axis of the crystal. The rocking curves about the (0010) Bragg reflection, with the X-ray incidence plane perpendicular to the defects, have a width approximately three times larger than that taken with an incidence plane parallel to the defects. This suggest that the planar defects separate zones of the crystal with slightly different orientations of the *c*-axis as have been observed by Koblischka et al. [17]. Therefore, the planar defects reported in this paper have the same crystallographic manifestation as those found in magneto-optical experiments.

One technique that has been proven to be very powerful in testing the *c*-axis superconducting correlation in BSCCO single crystals is the transverse ac permeability, $\mu_{ac}^{\perp}$ [29]. In these measurements a small ac magnetic field, h_{ac}, is applied parallel to the Cu–O planes while a static (DC) magnetic field is along the *c*-axis. Due to the strong anisotropy of the BSCCO most of the permeability signal is dominated by the inter-plane currents (*c*-axis currents) [29]. This is confirmed by the present measurements as we discuss below.

We have performed the $\mu_{ac}^{\perp}$ measurements with the ac field along the *a*-axis (parallel to the long side of the crystal and line defects) and along the *b*-axis (parallel to the short side of the crystal and perpendicular to the line defects). In the following we will call them the IN and OUT configurations respectively. In Fig. 3a we plot the real part of the permeability, $\mu'(T)$, for both configurations at zero DC field and 814 Oe. It is clear from this figure that μ'_{IN} presents a much broader transition on the zero field measurement and an almost parallel shift to lower temperatures in the "high' field data. In order to test if these features are product of size effects we have inverted numerically the data for the OUT configuration using the expression [30]:

$$\mu_{ac} = \frac{2\lambda_{ac}}{d} tanh\,(\frac{d}{2\lambda_{ac}})$$

valid for an infinite superconducting slab of thickness *d*, with λ_{ac} being the magnetic penetration depth, obtaining $(2\lambda_{ac}(T))/(d)$ for each field. Then we have divided this number by 1.5 (ratio between long and short sides of the crystal) and reconstructed μ_{ac}. The results of these calculations are shown in Fig. 3b. The coincidence between the data for both configurations at zero field and at high fields is evident. Note that the only assumption is the geometrical factor, independently of the temperature dependence of the penetration depth. With this data we can deduce a value for the London penetration depth $\lambda_c(0) \cong 100\,\mu m$ although there is a rather large uncertainty introduced by a non exact normalization of $\mu'(0)$. This simple numerical inversion demonstrates that size effects are important in this kind of experiments and that the relevant quantities are $\lambda_c(T)$, and the width of the sample (not the thickness) at least for the high temperature range.

Using these two measurement configurations (IN and OUT) we are also changing the relative orientation of the excitation field, h_{ac}, with respect to the defects. We will

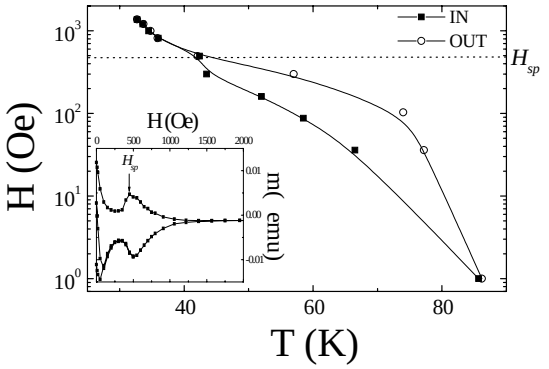

Fig. 5. H–T phase diagram. Solid squares: position of the maxima in μ''_{IN}; open circles maxima in μ''_{OUT}. Dotted line: second peak field. Inset: magnetization loop at 30 K indicating the second peak magnetic field.

use this technique to explore in-plane anisotropic pinning potentials as was done previously for twined YBCO single crystals [4].

In Fig. 4 we plot the $\mu'(T)$ for 36, 300 and 993 Oe after correcting by the size effect as noted above. It is clear from this figure that there is a different response between both configurations for a certain range of fields and temperatures. It has been found [8,11,31] that there is a region in the H–T phase diagram, delimited by the first order transition line, [11] the *second peak* [8,31] and the 0D line [9,32], where vortices behave as 3D objects. In contrast in the rest of the phase diagram the vortex ensemble responds either as a 2D liquid, a quasi-2D solid, or as a fully pinned vortex state. Of all these phases the only one which could interact effectively with a *c*-axis correlated planar defect is the 3D one, in full

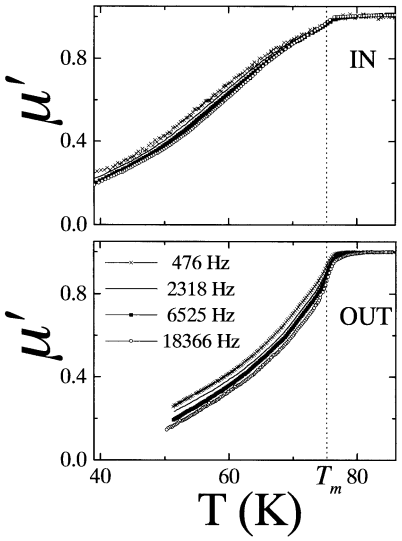

Fig. 6. $\mu'_{IN}(T)$ and $\mu'_{OUT}(T)$ for a magnetic field of 103 Oe measured at different frequencies.

agreement with our measurements shown in Fig. 4. When performing this kind of experiment on a vortex ensemble the elastic modulus that is basically tested is the tilt modulus, C_{44}. In the IN configuration the excitation stress on the vortices is forcing a tilt parallel to the planar defects. On the other hand with the OUT configuration vortices inside the defects will be pushed out of the pinning potential and vortices outside the defects will be pushed against the planar defects. As a consequence the anisotropic pinning potential produces an anisotropic C_{44} represented by the difference in the μ' data measured. In the 2D or quasi 2D phases the single vortex C_{44} is vanishingly small and so is its change by any *c*-axis correlated defect.

In Fig. 5 we plot the position of the peak in the imaginary part of the ac permeability μ'' for both configurations together with the position of the second peak measured in the same sample with DC magnetization loops (as shown in the inset). This figure clearly demonstrates that the planar defects are effective only in the 3D vortex regime, providing a crosscheck that the defects are correlated along the *c*-axis.

Now we turn to the effect of the correlated defects on the nature of the solid–liquid transition. Previous work [33,34] has shown that disorder modifies the first order transition introducing inhomogeneities in the critical temperature which produce an effective broadening of the transition in bulk measurements. In the transverse ac permeability measurements, the first order transition has been identified as a sudden and frequency independent increase in the real part of the susceptibility [11]. In Fig. 6 we plot the real part of the permeability, μ', as a function of the temperature, for an applied field of 103 Oe and for different excitation frequencies in both configurations. It is clear from the plot of the measurement performed in the IN configuration the existence of a temperature, T_m, where the ac permeability is frequency independent, very similar to that reported previously [11]. On the other hand there is a noticeable frequency dependence in the OUT measurements. We can only speculate about the origin of this frequency dependence. One possibility is that it arises from the activation of vortices pinned in the planar defects which are only excited in the OUT configuration.

3. Conclusions

In this work, we have shown that the naturally occurring planar defects in BSCCO single crystals have *c*-axis correlation deduced from Bitter decoration experiments and transverse permeability measurements in the superconducting mixed state. The vortex decorations show that these defects have a correlation length along the *c*-axis of at least 0.5 μm. Simultaneously, transverse permeability measurements show that they act as correlated defects only in the 3D vortex regime. The melting transition is still present but it is detected only when the excitation

field is along the defects. On the other hand, the importance of size effects in this kind of measurements has also been demonstrated.

Acknowledgements

Helpful discussions with F. de la Cruz and Dr Kitazawa are gratefully acknowledged. This work was partially supported by the Consejo Nacional de Investigaciones Científicas y Técnicas (CONICET- grant PIP 96/4207, Agencia Nacional de Promoción Científica y Tecnológica (grant 03-00061-01120) and Fundación Antorchas 1370/1-1118. J. A. H. and V. F. C. acknowledge support by CONICET through a scholarship.

References

[1] L. Civale, A.D. Marwick, T.K. Worthington, M.A. Kirk, J.R. Thompson, L. Krusin-Elbaum, Y. Sun, J.R. Clem, F. Holtzberg, Phys. Rev. Lett. 67 (1991) 648.
[2] S.A. Grigera, E. Morré, E. Osquiguil, C. Balseiro, G. Nieva, F. de la Cruz, Phys. Rev. Lett. 81 (1998) 2348.
[3] H. Pastoriza, S. Candia, G. Nieva, Phys. Rev. Lett. 83 (1999) 1026.
[4] J.A. Herbsommer, G. Nieva, J. Luzuriaga, Phys. Rev. B 61 (2000) 11745.
[5] W.K. Kwok, J.A. Frendrich, V.M. Vinokur, A.E. Koshelev, G.W. Crabtree, Phys. Rev. Lett. 76 (1996) 4596.
[6] V. Hardy, A. Wahl, S. Herbert, A. Ruyter, J. Provost, D. Groult, Ch. Simon, Phys. Rev. B 54 (1996) 656.
[7] M.V. Feigel'man, V.B. Geshkenbein, A.I. Larkin, Physica C 167 (1990) 177.
[8] L.I. Glazman, A.E. Koshelev, Phys. Rev. B 43 (1991) 7837.
[9] M.F. Goffman, J.A. Herbsommer, F. de la Cruz, T.W. Li, P.H. Kes, Phys. Rev. B 57 (1998) 3663.
[10] M.B. Gaifullin, Y. Matsuda, N. Chikumoto, J. Shimoyama, K. Kishio, Phys. Rev. Lett. 84 (2000) 2945.
[11] H. Pastoriza, M.F. Goffmann, A. Arribere, F. de la Cruz, Phys. Rev. Lett. 72 (1994) 2951.
[12] E. Zeldov, D. Majer, M. Konczykowski, V.B. Geshkenbein, V.M. Vinokur, H. Shtrikman, Nature (London) 375 (1995) 373.
[13] X.F. Zhang, G. Van Tandeloo, Philos. Mag. A 70 (1994) 549.
[14] M.V. Indenbom, C.J. van der Beek, V. Berseth, Th. Wolf, H. Berger, W. Benoit, J. Low, Temp. Phys. 105 (1996) 1529.
[15] I.-F. Tsu, J.-L. Wang, S.E. Babcock, A.A. Polyanskii, D.C. Larbalestier, K.E. Sickafus, Physica C 349 (2001) 8.
[16] C. Træholt, H.W. Zandbergen, T.W. Li, R.J. Drost, P.H. Kes, A.A. Menovsky, N.T. Hien, J.J.M. Franse, Physica C 290 (1997) 239.
[17] M.R. Koblischka, R.J. Wijngaarden, D.G. de Groot, R. Griessen, A.A. Menowski, T.W. Li, Physica C 249 (1995) 339.
[18] G. Yang, J.S. Abell, C.E. Gough, Physica C 341–348 (2000) 1091.
[19] Y. Fasano, J.A. Herbsommer, F. de la Cruz, Phys. Status Solidi (B) 215 (1999) 563.
[20] Y. Fasano, M. Menghini, F. de la Cruz, G. Nieva, Phys. Rev. B 62 (2000) 15183.
[21] E.E. Kaul, G. Nieva, Physica C 341–348 (2000) 1343.
[22] D.G. Grier, C.A. Murray, C.A. Bolle, P.L. Gammel, D.J. Bishop, D.B. Mitzi, A. Kapitulnik, Phys. Rev. Lett. 66 (1991) 2270.
[23] J.A. Herbsommer, G. Nieva, J. Luzuriaga, Phys. Rev. B 62 (2000) 678.
[24] J.A. Herbsommer, G. Nieva, J. Luzuriaga, Phys. Rev. B 62 (2000) 3534.
[25] P.L. Gammel, C.A. Durán, D.J. Bishop, V.G. Kogan, M. Ledvij, A. Yu Simonov, J.P. Rice, D.M. Ginsberg, Phys. Rev. Lett. 69 (1992) 3808.
[26] G.J. Dolan, G.V. Chandrashekhar, T.R. Dinger, C. Field, F. Holtzberg, Phys. Rev. Lett. 62 (1989) 827.
[27] I.V. Grigorieva, J.W. Steeds, K. Kasaki, Phys. Rev. B 48 (1993) 16865.
[28] I.V. Grigorieva, L.A. Gurevich, L. Ya Vinnikov, Physica C 195 (1992) 327.
[29] A. Arribere, H. Pastoriza, M.F. Goffman, F. de la Cruz, D.B. Mitzi, A. Kapitulnik, Phys. Rev. B 48 (1993) 7486.
[30] E.H. Brandt, Phys. Rev. Lett. 67 (1991) 2219.
[31] V.F. Correa, G. Nieva, F. de la Cruz, Phys. Rev. Lett. 87 (2001) 057003.
[32] M. Nideröst, A. Suter, P. Visani, A.C. Mota, G. Blatter, Phys. Rev. B 53 (1996) 9286.
[33] A. Oral, J.C. Barnard, S.J. Bending, S. Ooi, H. Taoka, T. Tamegai, M. Henini, Phys. Rev. B 56 (1997) R14295.
[34] A. Soibel, E. Zeldov, M. Rappaport, Y. Myasoedov, T. Tamegai, S. Ooi, M. Konczykowski, V.B. Geshkenbein, Nature 406 (2000) 282.